

1 **Lipid nanoparticle composition for adjuvant formulation modulates disease after influenza**
2 **virus infection in QIV vaccinated mice.**

3 Sonia Jangra^{1,2}, Alexander Lamoot³, Gagandeep Singh^{1,2}, Gabriel Laghlali^{1,2,3}, Yong Chen³,
4 Tingting Yz³, Adolfo García-Sastre^{1,2,4,5,6}, Bruno G. De Geest³, Michael Schotsaert^{1,2,7,8,*}

5

6 [*Michael.Schotsaert@mssm.edu](mailto:Michael.Schotsaert@mssm.edu) (+1 212 241 4847), corresponding author

7 ¹Department of Microbiology, Icahn School of Medicine at Mount Sinai New York, NY, USA

8 ²Global Health and Emerging Pathogens Institute, Icahn School of Medicine at Mount Sinai New
9 York, NY, USA

10 ³Department of Pharmaceutics, Ghent University, Ghent Belgium

11 ⁴Department of Medicine, Division of Infectious Diseases, Icahn School of Medicine at Mount Sinai
12 New York, NY, USA

13 ⁵The Tisch Cancer Institute, Icahn School of Medicine at Mount Sinai New York, NY, USA

14 ⁶Department of Pathology, Molecular and Cell-Based Medicine, Icahn School of Medicine at Mount
15 Sinai New York, NY, USA

16 ⁷ Icahn Genomics Institute, Icahn School of Medicine at Mount Sinai, New York, NY, USA

17 ⁸ Marc and Jennifer Lipschultz Precision Immunology Institute, Icahn School of Medicine at Mount
18 Sinai, New York, NY, USA

19

20 **Key words:** Influenza Vaccine, QIV, Adjuvant, Lipid nanoparticles, ionizable lipids, vaccine
21 formulations, T cell, Antibody Class Switching, IgG, cytokines.

22 **Abstract**

23 Adjuvants can enhance vaccine effectiveness of currently licensed influenza vaccines. We tested
24 influenza vaccination in a mouse model with two adjuvants: Sendai virus derived defective
25 interfering (SDI) RNA, a RIG-I agonist, and an amphiphilic imidazoquinoline (IMDQ-PEG-Chol),
26 TLR7/8 adjuvant. The negatively charged SDI RNA was formulated into lipid nanoparticles (LNPs)
27 facilitating the direct delivery of a RIG-I agonist to the cytosol. We have previously tested SDI and
28 IMDQ-PEG-Chol as standalone and combination adjuvants for influenza and SARS-CoV-2
29 vaccines. Here we tested two different ionizable lipids, K-Ac7-Dsa and S-Ac7-Dog, for LNP
30 formulations. The adjuvanticity of IMDQ-PEG-Chol with and without empty or SDI-loaded LNPs
31 was validated in a licensed vaccine setting (quadrivalent influenza vaccine or QIV) against H1N1
32 influenza virus, showing robust induction of antibody titres and T cell responses. Depending on the

33 adjuvant combination and LNP lipid composition (K-Ac7-Dsa or S-Ac7-Dog lipids), humoral and
34 cellular vaccine responses could be tailored towards type 1 or type 2 host responses with specific
35 cytokine profiles that correlated with protection during viral infection. The extent of protection
36 conferred by different vaccine/LNP/adjuvant combinations was examined against challenge with the
37 vaccine-matching strain of H1N1 influenza A virus. Groups that received either LNP formulated
38 with SDI, IMDQ-PEG-Chol or both showed very low levels of viral replication in their lungs at five
39 days post virus infection. LNP ionizable lipid composition as well as loading (empty versus SDI)
40 also skewed host responses to infection, as reflected in the cytokine and chemokine levels in lungs of
41 vaccinated animals upon infection. These studies show the potential of LNPs as adjuvant delivery
42 vehicles for licensed vaccines and illustrate the importance of LNP composition for subsequent host
43 responses to infection, an important point of consideration for vaccine safety.

44

45

46

47 Introduction

48 After decades of research into influenza virus vaccines, the respiratory virus is still a major global
49 health concern causing thousands of cases of severe medical illness in humans every year. Several
50 licensed influenza vaccine candidates, including recombinant, inactivated and split influenza
51 vaccines, have been developed and eventually licensed for use in the human population^{1,2}. Despite
52 the availability of licensed vaccines, the need to update and vaccinate people every year remains a
53 challenge as the circulating influenza viruses can escape host immunity provided by antibodies that
54 target the immunodominant but ever-changing antigenic sites on the hemagglutinin (HA) protein³⁻⁵.
55 Vaccination against both seasonal Influenza A (IAV) and influenza B (IBV) has been effective in
56 controlling virus-related disease severities. However, the protection provided by humoral immunity
57 induced by these vaccines is reported as antigenically constricted and short term. Moreover, the
58 vaccine-induced neutralizing antibody titres drop over time, rendering the immunity less effective
59 against an antigenically different strain of virus in the subsequent seasons⁶⁻⁸. Therefore, to combat
60 the need of a seasonal vaccine, a better cost-effective approach is required in vaccine development
61 which can provide a broader and long-term immune response that lasts for multiple seasons.

62 Inactivated split virus vaccines, including trivalent inactivated vaccines (TIV) and quadrivalent
63 inactivated vaccines (QIV), are most commonly used influenza vaccines. TIV comprises of two IAV
64 strains, one each of H1N1 and H3N2 subtype, and one IBV component, while QIV consists of two
65 IAV and two IBV strains components (representing the Yamagata and Victoria lineages)^{9,10}. These
66 vaccines can induce strain-specific antibody responses with high serum IgG levels *in vivo* but are
67 poor inducers of cell-mediated immunity and therefore, provide limited protection against
68 antigenically drifted virus strains. Due to the continuous acquisition of mutations in antigenic sites of
69 the viral hemagglutinin, the protective effect of currently licensed seasonal influenza virus vaccines
70 is time confined.

71 Novel vaccine concepts that aim at inducing broader, long-lasting immunity against influenza virus
72 infection are based on enhancing vaccine- induced B and T cell responses which can recognize
73 multiple antigens from vaccine components, with special focus on targeting the conserved viral
74 epitopes. While natural infection typically results in the induction of type 1 responses, characterised
75 by Th1 and in BALB/c mice class switching to serum IgG2a antibodies to clear viral infection¹¹⁻¹³,
76 inactivated split virus influenza vaccines typically induce high IgG1 levels correlating with Th2-type
77 immune response¹⁴⁻¹⁶. Therefore, many studies, including our recently published study¹⁷, have been
78 focusing on combining commercially available vaccines with specific adjuvants to specifically direct

79 responses to IgG2a or IgG1, hence inducing Th1/Th2 responses¹⁸⁻²¹. Eventually, an efficiently
80 balanced humoral response with enhanced T cell activation post-vaccination is desired to be
81 protective.

82 Lipid nanoparticles (LNPs) are non-viral vectors that are widely used in formulating vaccines and/or
83 adjuvants to enhance their antigenicity and improve immune responses^{22,23}. LNPs have already
84 shown promising outcomes in formulating antigen-encoding mRNA, such as SARA-CoV-2 mRNA
85 vaccines²⁴. These mRNA vaccine-LNP formulations have also successfully demonstrated the role of
86 LNP-based vaccine platform for an efficient induction of humoral and cell-mediated immunity.
87 Moreover, LNPs can also be used for formulating molecular adjuvants, such as RIG-I or TLR
88 agonists, and facilitate uptake by actively phagocytosing innate immune cell subsets²⁵. Nevertheless,
89 the composition of LNP is crucial to achieve the optimal uptake by innate immune cells and efficient
90 humoral responses. A typical LNP consists of four main components: an ionizable lipid, a
91 phospholipid, cholesterol moiety and polyethylene-glycol (PEG)-lipid. The ionizable lipids consist of
92 ionizable positively charged lipids that can effectively interact with negatively charged mRNA
93 molecules. Phospholipids and cholesterol provide structural stability to LNPs and facilitate
94 endosomal escape, thus enhancing efficient delivery of mRNA into the cytosol of cells. The PEG
95 lipids prolong the circulation of LNPs consisting of vaccines/adjuvants in circulation by increasing
96 their half-life. Additionally, the surface molecules of LNPs can also be modified to target specific
97 innate immune cells and facilitate uptake for efficient antigen presentation^{23,25-27}. Overall, LNPs
98 present as an efficient *in vivo* vaccine-adjuvant delivery system.

99 In this study, we investigated and compared the efficiency of two LNP formulations, consisting of
100 different ionizable cationic lipids, in inducing both humoral and cell mediated immune responses in a
101 mouse model receiving a single shot of QIV from 2018-19 influenza season, with and without
102 adjuvants, individually or in combination. Specifically, we used an *in vitro* transcribed Sendai virus
103 defective-interfering RNA^{17,28,29} (SDI-RNA; a RIG-I agonist; negatively charged and hence
104 encapsulated into LNPs) and an amphiphilic imidazoquinoline conjugate^{17,30} (IMDQ-PEG-Chol; a
105 modified TLR7/8 agonist with enhanced safety profile and lymph node-draining properties),
106 previously characterized and tested by our groups, as adjuvants. Vaccine-induced antibody and T cell
107 responses were characterized and further correlated with lung cytokine profiles and extent of
108 protection against lethal challenge of a matching strain to H1N1 component of QIV:
109 A/Singapore/GP1908/2015 (IVR-180). We observed adjuvant-specific differences in B- and T- cell
110 responses, which were not only driven by the presence of different adjuvants (SDI RNA and/or

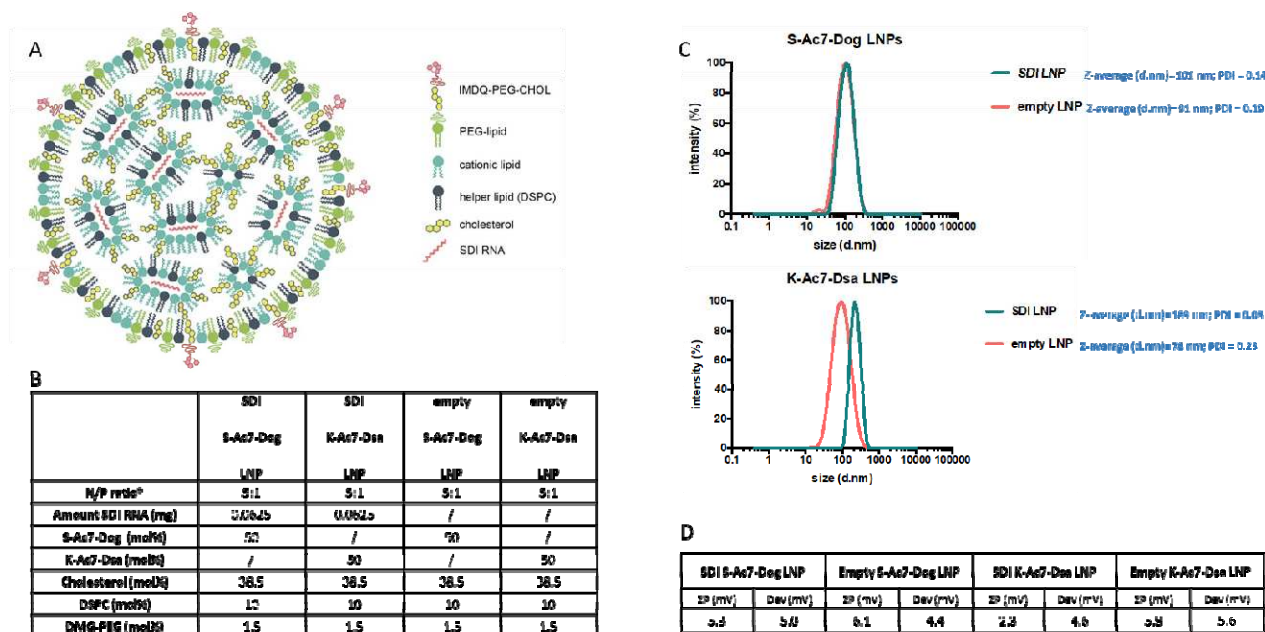
111 IMDQ-PEG-CHOL) but also depended on the type of ionizable/cationic lipid composition of the
112 LNPs.

113

114 **Results**

115 **Preparation and characterization of LNPs:**

116 Two LNP formulations were prepared by mixing an aqueous solution containing the *in vitro*
117 transcribed SDI-RNA (or SDI) with an ethanolic solution containing (1) ionizable lipids, either K-
118 Ac7-Dsa (comprising a ketal bond) or S-Ac7-Dog (comprising a disulfide bond; chemical structure
119 outlined in supplementary Fig 1), to interact with negatively charged SDI and mediate endosomal
120 escape; (2) cholesterol, for structural stability; (3) dioleoylphosphatidylethanolamine (DOPE)
121 phospholipid, as helper lipids to aid in nanoparticle formation; (4) 1,2-distearoyl-rac-glycero-3-
122 methylpolyethylene glycol (DSG-PEG; 2kDa PEG) to provide steric hinderance and thus avoiding
123 aggregation and promoting mobility *in vivo*. The structure and composition of LNP incorporating
124 SDI-RNA is schematically represented in Fig 1A and B, respectively. The molar ratio of ionizable
125 lipid (K-Ac7-Dsa or S-Ac7-Dog): cholesterol: DOPE: DSG-PEG was chosen to be 50:38.5:10:1.5,
126 based on literature. Empty LNP, that did not contain SDI, were prepared as control and hence
127 referred to as LNP(-). Both LNPs encapsulating SDI (S-Ac7-Dog(SDI) and K-Ac7-Dsa (SDI)) and
128 corresponding control empty LNPs (S-Ac7-Dog(-) and K-Ac7-Dsa (-)) were fabricated and
129 characterized for their size and zeta potential (Fig 1C and 1D). While K-Ac7-Dsa(-) and K-Ac7-
130 Dsa(SDI) LNPs showed some differences in their size (78 and 189 nm respectively), the S-Ac7-
131 Dog(-) and S-Ac7-Dog(SDI) LNPs showed similar size distributions (91 and 101 nm respectively)
132 with low polydispersity indices (PDI< 0.25; as shown in Fig 1C) and a positive zeta potential (ZP)
133 around 4-6.5 mV at physiological pH (Fig 1D).



135 **Figure 1. Structure and characterization of LNPs consisting of K-Ac7-Dsa or S-Ac7-Dog lipids.**
136 (A) Diagrammatic representation of LNP structure encapsulating SDI (B) Composition ratio of
137 different components of LNPs, with and without SDI (C) Intensity-based size distribution curves
138 measured by Dynamic Light Scattering (DLS) of empty and SDI-incorporating S-Ac7-Dog and K-
139 Ac7-Dsa LNP formulations (D) Summarizing table of the LNPs zeta potential measured by
140 Electrophoretic Light Scattering (ELS).

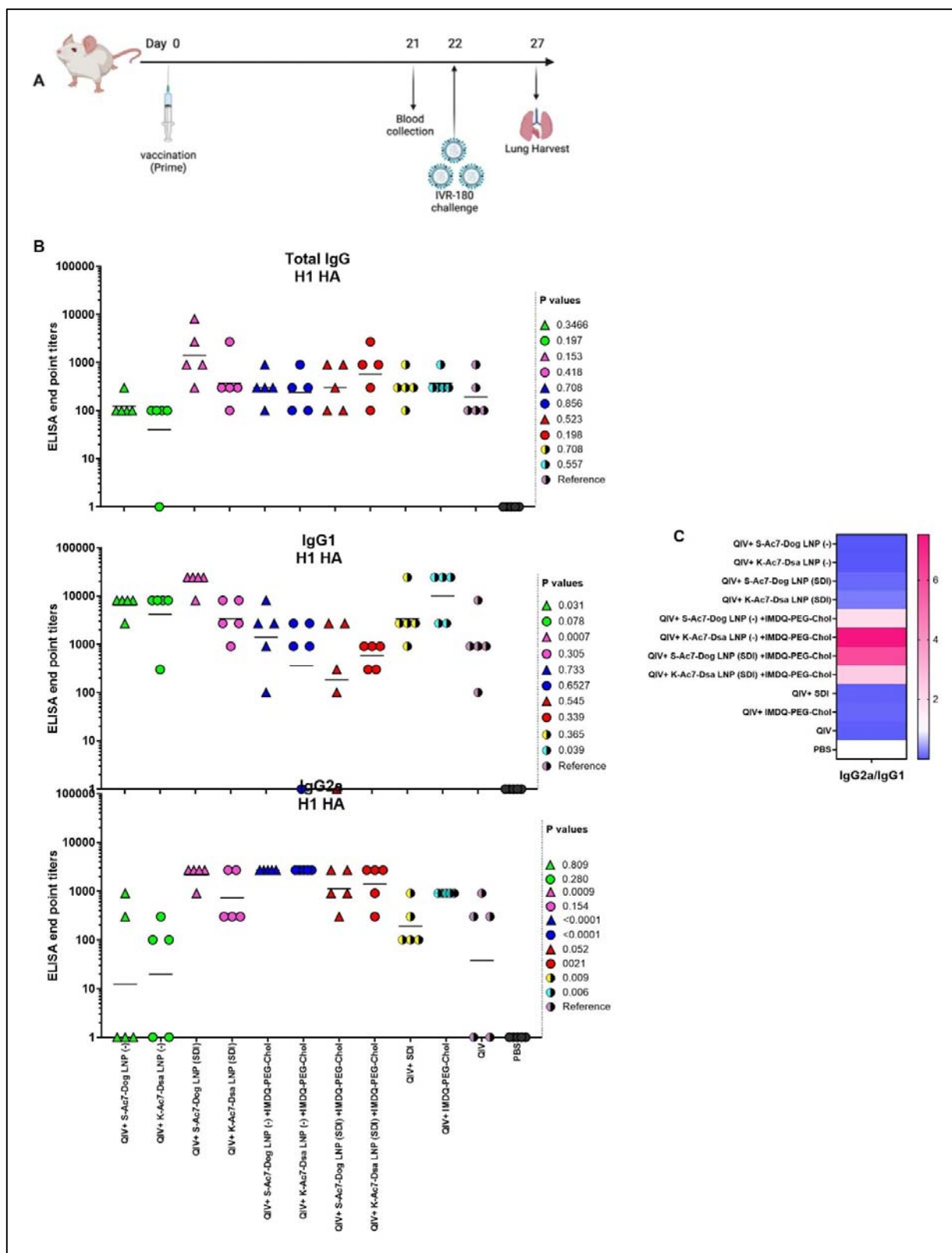
141

142 **LNP formulations with adjuvanted QIV define IgG subtype profile, with S-Ac7-Dog LNPs**
143 **inducing higher antibody titers than K-Ac7-Dsa LNPs:**

144 We evaluated the potential of empty and SDI-incorporating S-Ac7-Dog and K-Ac7-Dsa LNPs to
145 adjuvant a licensed quadrivalent influenza vaccine (QIV), with and without combination with
146 IMDQ-PEG-Chol adjuvant, using our previously well-established preclinical vaccination-infection
147 animal model. The study is outlined in Fig 2A. We vaccinated 6-8-week female BALB/c mice with
148 unadjuvanted QIV or in combination with SDI or IMDQ-PEG-Chol or both, while mock animals
149 received PBS. We further tested the adjuvant effect for QIV upon co-administration of SDI and/or
150 IMDQ-PEG-Chol combined with one of the two LNPs containing different cationic lipids (S-Ac7-
151 Dog or K-Ac7-Dsa) as described in previous section. LNPs were either empty (-) or had SDI
152 incorporated. The rationale of this set up is that LNP-formulated SDI can, besides endosomes, also
153 be delivered to the cytosol, thereby promoting more efficient RIG-I mediated innate immune
154 sensing. On the other hand, IMDQ-PEG-Chol is expected to incorporate efficiently in LNPs via its
155 cholesterol moiety. The animals were vaccinated only once via the intramuscular (IM) route. The
156 serum collected 3 weeks post-vaccination was examined for the presence of H1 HA-specific IgG
157 antibodies using enzyme-linked immunosorbent assay (ELISA) for total IgG, IgG1 and IgG2a (Fig.
158 2b).

159 No antibody titers were detected in the serum from mock PBS group. The group which received
160 unadjuvanted QIV was used as the reference to compare the IgG responses of other groups. QIV
161 formulated with S-Ac7-Dog LNP (-) or K-Ac7-Dsa LNP(-), corresponding to empty S-Ac7-Dog and
162 empty K-Ac7-Dsa LNPs respectively, showed higher IgG1 titers but lowest IgG2a titers compared
163 with the corresponding S-Ac7-Dog LNP(SDI) or K-Ac7-Dsa LNP(SDI) groups (Fig 2B and
164 supplementary Fig 2), thereby illustrating the intrinsic adjuvant effect of LNPs. Additionally, QIV
165 formulated with SDI-incorporated LNPs (S-Ac7-Dog LNP(SDI) and K-Ac7-Dsa LNP(SDI)) can
166 induce a balanced IgG1 and IgG2a antibody response. Overall, the total IgG levels were found

167 similar among all adjuvanted and LNP-formulated groups post-prime vaccination. However, the S-
168 Ac7-Dog LNP(SDI) seemed to be induce slightly higher total IgG slightly compared to K-Ac7-Dsa
169 LNP (SDI) in corresponding SDI \pm IMDQ-PEG-Chol combination adjuvanted groups. A similar
170 observation was made for IgG1 antibody titers with S-Ac7-Dog LNPs inducing higher IgG1 titers
171 than respective K-Ac7-Dsa LNP groups. Consistent with our previous findings¹⁷, IMDQ-PEG-Chol
172 administration, with either of empty or SDI-incorporated S-Ac7-Dog or K-Ac7-Dsa LNPs, skews the
173 antibody responses towards IgG2a with a significant reduction in IgG1 titers (Fig 2C). QIV+SDI and
174 QIV+IMDQ-PEG-Chol groups, with no LNP formulations, were used as control vaccination groups
175 for the study and to correlate with our previous study.



176

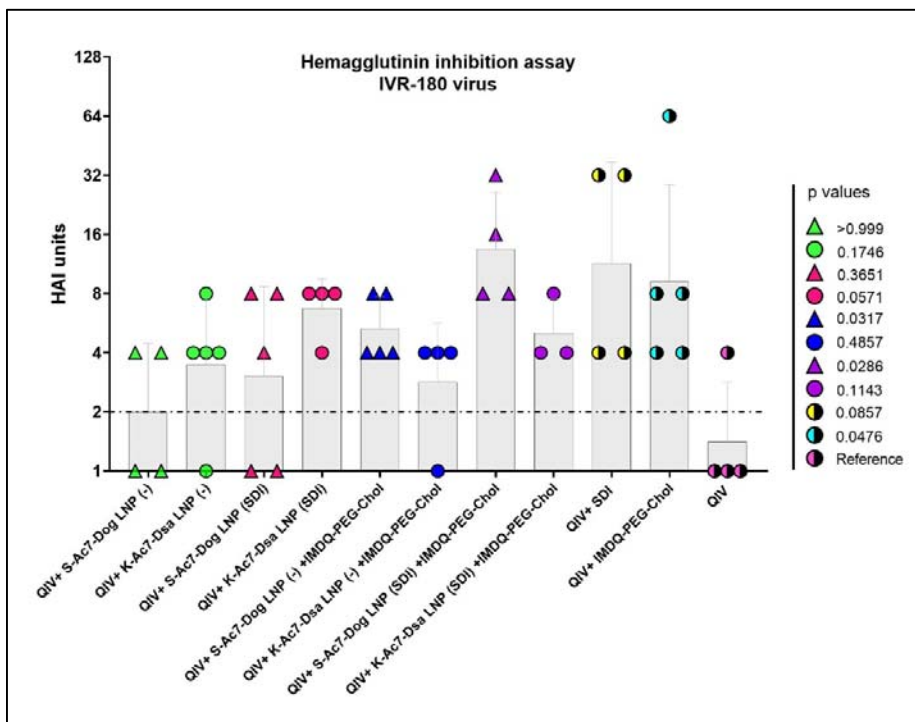
177 **Figure 2: S-Ac7-Dog (- or SDI) and K-ac7-Dsa (- or SDI) in combination with IMDQ-PEG-**
 178 **Chol define IgG subtype profile: (A) Study outline (B) Graphs showing ELISA end point titers**

179 calculated based on OD450 ELISA values against serum dilutions for total IgG, IgG1 and IgG2a
180 (n=5 per group), represented as geometric mean. The statistical analysis was performed using
181 unpaired T test and the p values shown are calculated in reference to the unadjuvanted QIV group
182 which received neither adjuvant nor LNP formulations. (C) Heatmap showing the ratio of end point
183 titers of IgG2a to IgG1 and represented as geometric mean of IgG2a/IgG1 ratios for all animal in
184 each group.

185

186 **QIV adjuvanted with IMDQ-PEG-Chol exhibit a better control over virus neutralization when
187 formulated in S-Kc7-Dog LNPs than K-Ac7-Dsa LNPs:**

188 Neutralizing antibodies are important defense mechanisms during viral infection. These antibodies
189 bind to the viral antigens and thereby block the viral attachment to cells. As a surrogate for virus
190 neutralizing antibody levels, we performed hemagglutinin inhibition (HAI) assays with post-
191 vaccination sera collected from all vaccinated animals at 3 weeks post vaccination. As shown in Fig
192 3, the mice that received unadjuvanted QIV showed low HAI titers which were not significantly
193 different from the groups that received QIV formulated in either empty or SDI-containing S-Ac7-
194 Dog or K-Ac7-Dsa LNPs. The group administered with QIV+IMDQ-PEG-Chol, without LNP
195 formulations, showed significantly higher HAI titers compared with unadjuvanted QIV group. HAI
196 titers were significantly higher for the groups that received empty or SDI-containing S-Ac7-Dog in
197 the LNP formulation when combined with IMDQ-PEG-Chol adjuvant. However, the corresponding
198 K-Ac7-Dsa LNP-formulated groups did not show any significant differences in HAI titers compared
199 with unadjuvanted or unformulated QIV group.



200

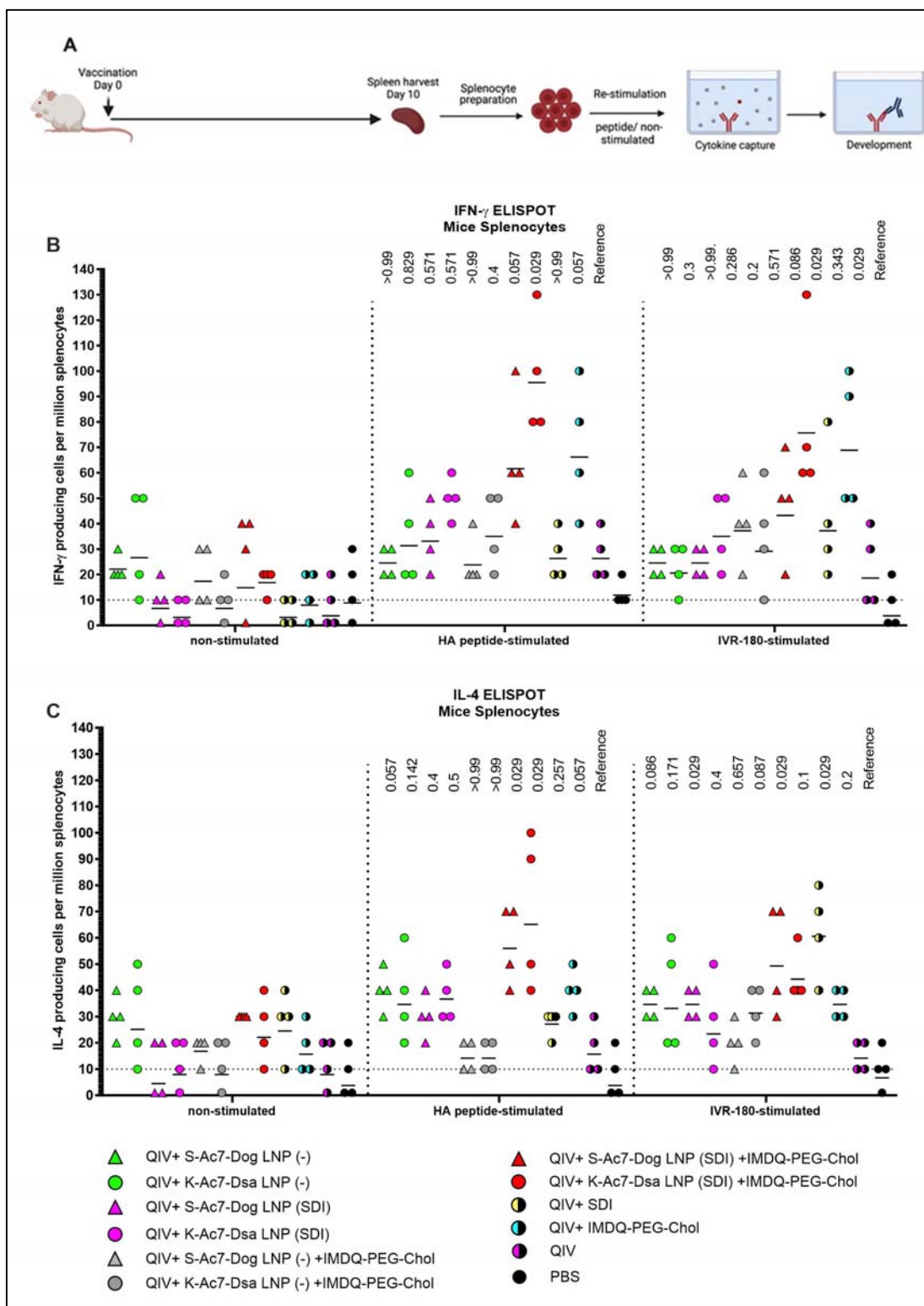
201 **Figure 3: QIV adjuvanted with IMDQ-PEG-Chol exhibits a better control over virus infection**
202 **when formulated in S-Kc7-Dog LNP:** The sera collected from all vaccinated animals 3 weeks
203 post-vaccination was tested for HAI titers, using 4 HA units of IVR-180 virus. The HAI titers are
204 represented as geometric mean \pm geometric SD for n=4 animals per group. The samples with un-
205 detectable HAI titers were set as 1 and the limit of detection was set to 2, corresponding to the lowest
206 detectable HAI units. The statistical analysis was performed using two-sided Mann Whitney U test.
207 The p values shown are calculated in reference to the QIV group which received neither adjuvant nor
208 LNP formulations.

209

210 **QIV formulated in either of SDI-containing S-Ac7-Dog and K-Ac7-Dsa LNP efficiently induce**
211 **T cells responses when combined with IMDQ-PEG-Chol:**

212 Helper CD4+ and cytotoxic CD8+ T cells play an important part in vaccination-mediated humoral
213 and cellular responses by facilitating Ig class switch during B cell maturation and direct killing of
214 infected cells, respectively. T cells can recognize foreign antigens presented on the major
215 histocompatibility complex (MHC) molecules on infected cells followed by release of various
216 cytokines, including IFN- γ and IL-4, two major cytokines corresponding to helper type-1
217 (Th1) and type-2 (Th2) T cells, respectively. IFN- γ and IL-4 can modulate class switching of B cells
218 to IgG2a or IgG1¹⁹. To study the correlation between the two cytokines and antibody responses in

219 our vaccination model, we examined the release of IFN- γ and IL-4 from splenocytes obtained from
220 the mice 10 days post-vaccination (outlined in Fig 4A), in presence and absence of specific antigen
221 (IVR-180 virus or H1 HA peptide) using enzyme-linked immunosorbent spot (ELISpot) assays.
222 As shown in Fig 4B and C, antigen-specific IFN- γ (Fig 4B) or IL-4 (Fig 4C) release from the
223 splenocytes was very low in the absence of a stimulant, except for QIV+S-Ac7-Dog(-) or QIV+K-
224 Ac7-Dsa(-) groups suggesting a basal level of non-specific stimulation after vaccination by the
225 empty LNPs. Upon stimulation with specific H1-HA peptide or IVR-180 virus, the number of
226 splenocytes producing antigen-specific IFN- γ as well as IL-4 were found to be higher
227 in the mice that received QIV+IMDQ-PEG-Chol formulated in S-Ac7-Dog(SDI) or K-Ac7-
228 Dsa(SDI) LNPs, suggesting an induction in both Th1 and Th2 immune response. The group
229 administered with QIV+IMDQ-PEG-Chol, without LNP formulations, showed high IFN- γ release
230 compared with unadjuvanted QIV group, consistent with our previous study. Mice that received QIV
231 only were used as a reference for statistical comparison.



232

233 **Figure 4: QIV formulated in S-Ac7-Dog(SDI) and K-Ac7-Dsa(SDI) LNPs efficiently induce T**
 234 **cell responses when combined with IMDQ-PEG-Chol: (A) Experiment outline (B,C) 6-8 weeks**
 235 **BALB/c mice were vaccinated with QIV with and without IMDQ-PEG-Chol and formulated into S-**

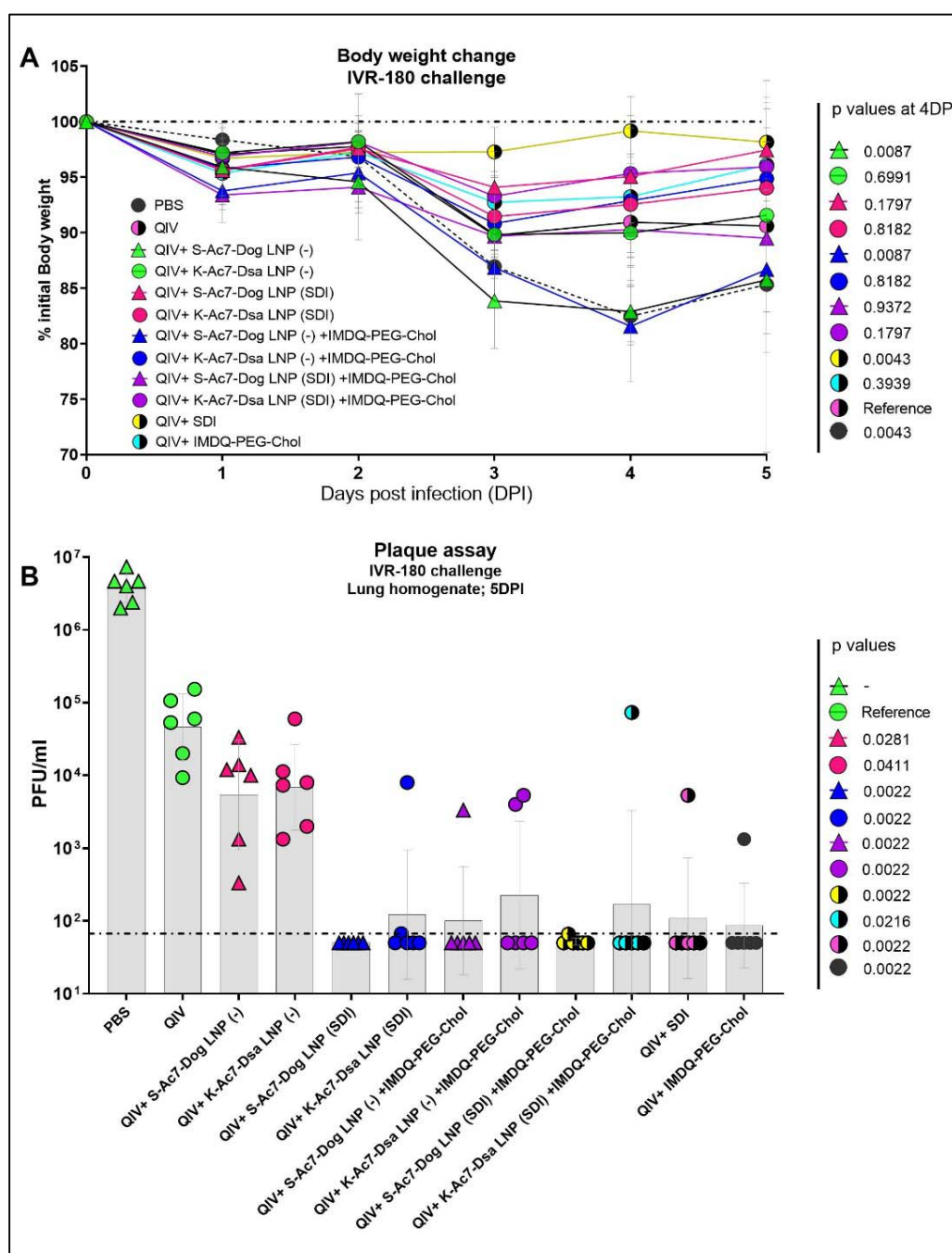
236 Ac7-Dog(- or SDI) or K-Ac7-Dsa(- or SDI) LNPs. The spleens were harvested 10 days post-
237 vaccination to examine the T cell activation by IFN- γ (**B**) and IL-4 (**C**) ELIsots, upon restimulation
238 with H1-HA short-overlapping peptides or live IVR-180 (A/Singapore/GP1908/2015 H1N1) virus.
239 The results are represented as IFN- γ or IL-4 producing cells per million splenocytes (geometric mean
240 \pm geometric SD) for n=4 animals per group. The cut-off was set to 10 which indicates one spot in
241 any well. The wells with no spots were given the value 1. The statistical analysis was performed
242 using two-sided Mann Whitney U test and the p values shown are calculated in reference to the
243 respective unadjuvanted QIV group.

244

245 **S-Ac7-Dog and K-Ac7-Dsa LNP formulations with SDI and/or IMDQ-PEG-Chol potentiates**
246 **QIV-mediated protection against a lethal viral challenge with homologous influenza virus:**
247 To further correlate B and T cell responses with the extent of protection, all vaccinated and un-
248 vaccinated mice were challenged with 100 times 50% lethal dose of IVR-180 virus (18000 PFU per
249 animal). A single dose of vaccination was found effective in conferring protection from severe
250 morbidity in challenged animals compared with mock-challenged mice by day 5 of infection. As
251 shown in Fig 5A, the groups receiving unadjuvanted QIV and QIV with K-Ac7-Dsa(- or SDI) LNPs
252 showed less than 10% body weight loss over 5 days post infection. The unvaccinated PBS group lost
253 approximately 20% body weight by 4DPI. Interestingly, the mice vaccinated with S-Ac7-Dog (-),
254 irrespective of combination with IMDQ-PEG-Chol, showed drastic weight loss over 5 days, almost
255 comparable to the unvaccinated PBS group. This is especially important to note because the same S-
256 Ac7-Dog LNPs incorporating SDI did not show such extensive weight loss in vaccinated/challenged
257 animals, suggesting higher morbidity in virus infected lungs in case of empty S-Ac7-Dog LNP
258 formulations.

259 Irrespective of the body weight loss differences attributed by LNPs, all groups which received
260 adjuvanted QIV showed lower amount of replicating virus in their lungs 5 days post-infection (Fig
261 5B), compared with the unadjuvanted QIV group. QIV formulated in either of the two empty LNPs
262 (S-Ac7-Dog(- or K-Ac7-Dsa(-)) did not provide significant protection compared with unadjuvanted
263 QIV group, contrary to the higher IgG1 induction. The groups that received QIV with either of S-
264 Ac7-Dog(- or SDI) or K-Ac7-Dsa(- or SDI) LNPs, irrespective of IMDQ-PEG-Chol combination,
265 resulted in significantly better control of lung virus replication, with very low detectable titers in
266 their lungs and therefore, correlated with enhanced vaccine responses observed in mice.
267 Interestingly, S-Ac7-Dog LNPs seemed to provide more protection compared to K-Ac7-Dsa LNPs in
268 animals when compared between corresponding adjuvant groups.

269



271 **Figure 5: QIV formulated in S-Ac7-Dog(SDI) and K-Ac7-Dsa(SDI) LNPs protects the**
272 **vaccinated animals against a lethal dose of IVR-180, irrespective of combination with IMDQ-**
273 **PEG-Chol:** All unvaccinated and QIV± IMDQ-PEG-Chol ± S-Ac7-Dog(SDI) or K-Ac7-Dsa(SDI)
274 vaccinated animals were intranasally challenged with 100LD₅₀ (18000 PFU per animal) of IVR-180
275 virus. (A) The body weight of each animal in all groups was recorded every day until the day of
276 harvest and represented as percentage initial body weight for each group (n=6) (geometric mean

277 \pm geometric SD). **(B)** The viral lung titers were quantified at 5 days post infection by plaque assays
278 on pre-seeded MDCK cells and are represented as Plaque \square forming \square unit (PFU)/ml for n=6 animals
279 per group (geometric mean \pm geometric SD). Each data point represents one animal in the respective
280 group. Statistical analysis was performed using two-sided Mann Whitney U test. The p values shown
281 are calculated in reference to the unadjuvanted QIV group which received neither adjuvant nor LNP
282 formulations.

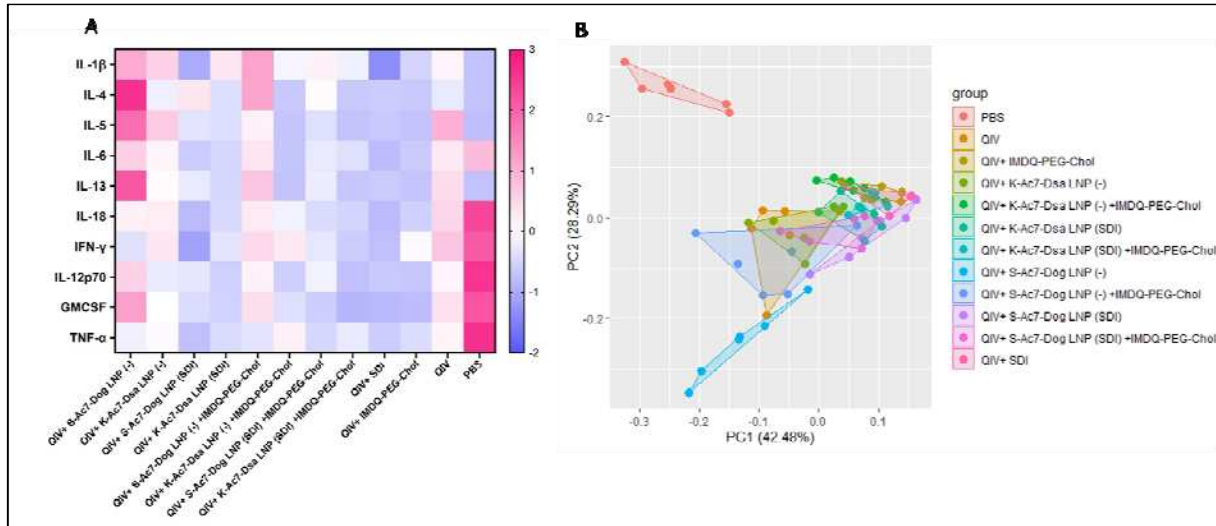
283

284 **Incorporation of SDI as an adjuvant improves the cytokine profile in lungs of infected animals
285 causing less morbidity as compared to empty S-Ac7-Dog LNP formulations:**

286 The body weight data over 5 days post infection suggested that the administration of empty S-Ac7-
287 Dog LNP as vaccine \pm adjuvant formulation was, although protective, did not provide protection
288 from body weight loss compared to PBS-vaccinated control mice. The lungs of all infected animals
289 were examined for their cytokine profiles 5 days post infection. As shown in Fig 6 and
290 supplementary Fig 3, the cytokine profiles in the infected lungs of animals from vaccinated or
291 unvaccinated/PBS groups were different. The PBS group showed high levels of inflammatory
292 cytokines including IL-6, IL-18, IL-12 p70, IFN- γ , TNF- α as well as chemokine GMCSF which may
293 suggest enhanced vascular permeability and increased infiltration of innate immune cells in response
294 to infection in unvaccinated animals. As shown in Fig 6A, these cytokine levels were significantly
295 lower in all vaccinated groups, implying a better control over inflammation and morbidity in
296 response to the virus. Some of the cytokines were very low in PBS group, especially the signatures
297 for T cell responses such as IL-4, IL-5 and IL-13, which is in line with the typical type 1 skewed host
298 immune response to influenza infection. Interestingly, pro-inflammatory cytokines and chemokines,
299 including IL-1 β , GMCSF, and the type 2 cytokines IL-4, IL-5, IL-6, IL-13 were significantly
300 elevated in unadjuvanted QIV and QIV \pm IMDQ-PEG-Chol formulated with empty LNPs. This was
301 not the case for the corresponding groups with LNP(SDI), especially for those LNP groups with S-
302 Ac7-Dog lipids. The PCA plot in Fig 6B clusters different vaccinated and unvaccinated groups based
303 on their differences in production of inflammatory cytokines and chemokines in lungs post-infection.
304 The unvaccinated PBS group clusters far away from all vaccinated animals corresponding to high
305 inflammation and chemokine production in lungs post infection with lower interleukins. Besides, the
306 QIV+ S-Ac7-Dog(-) vaccinated group clustered separately from the other vaccinated groups.
307 Additionally, the group that received QIV+ S-Ac7-Dog(-) combined with IMDQ-PEG-Chol is
308 clustered together with unadjuvanted QIV, suggesting that the use of empty S-Ac7-Dog is

309 disadvantageous as it reduces the protective effect of IMDQ-PEG-Chol when used without any lipid
310 formulation. The other vaccinated groups showing low inflammation in lungs clustered together.

311



312

313 **Figure 6: Heatmap showing cytokine profile in lungs of vaccinated mice upon intranasal
314 challenge with IVR-180:** All unvaccinated and vaccinated animals were intranasally challenged
315 with 18000 PFU of IVR-180 virus. The lungs were collected at 5 days post infection and the
316 cytokine levels were quantified by multiplex ELISA. Levels of IL-1 β , IL-5, IL-13, TNF- α , IL-12
317 p70, IL-4, IL-6, IFN- γ , IL-18 and GMCSF, for n=6 animals per group are represented as median of
318 z-scores (A) and PCA plots (B) for all animals in each group.

319

320

321

322

323

324

325 **Discussion**

326 Quadrivalent inactivated influenza vaccines (QIV), consisting of two influenza A (IAV) and two
327 influenza B (IBV) virus strain components and one of the licensed influenza vaccines, are modified
328 and administered annually to provide immunity against circulating influenza viruses in human
329 population. Several studies have been focussed on improving these split vaccines' efficiency by
330 combining them with adjuvants, including our recent study on RIG-I and TLR7/8 agonists as
331 adjuvants for QIV. Then again, the stability of these vaccines \pm adjuvants (such as SDI RNA; a RIG-I
332 agonist) and their efficient *in vivo* delivery is still challenging. To overcome this, lipid nanoparticles
333 (LNPs) have emerged as promising vehicles for *in vivo* delivery systems. Their ability to
334 encapsulate, stably carry and efficiently deliver the molecules-of-interest has provided an effective
335 platform in pharmaceutical as well as vaccine fields. One such example is highly efficient current
336 mRNA vaccines for SARS-CoV-2 which use LNP-based formulations²⁴. Nevertheless, these
337 vaccines still need multiple booster doses to be sufficiently effective against emerging virus strains
338 and therefore are limited in inducing an antigenically broader immune responses. Therefore, the
339 LNPs doses and composition need to be tailored together with the vaccine and/or adjuvant
340 combinations, in order to get the desired vaccination outcomes in terms of both humoral and cellular
341 responses, besides providing protection against viral infections^{22,25}.

342 In this study, we tested adjuvant formulations for QIV (2018-19 season; with A/
343 Singapore/GP1908/2015 IVR-180 (H1N1) as one of the two IAV components) with two different
344 LNP formulations using either S-Ac7-Dog or K-Ac7-Dsa cationic lipids. Since the lipids are
345 positively charged, they can stably interact with negatively charged biomolecules. The vaccine-LNP
346 combinations were further adjuvanted with either one or both of RIG-I and TLR7/8 agonists (SDI-
347 RNA and IMDQ-PEG-Chol, respectively), to explore the outcomes of the vaccine \pm adjuvant \pm LNP
348 formulations in context of antibody responses, antibody class switching, T cell responses, protection
349 against a lethal dose of IVR-180 virus and inflammatory responses in the infected lungs.

350 The unadjuvanted QIV vaccine induces modest serum IgG1 and IgG2a titres as well as low
351 hemagglutinin inhibition titres 3 weeks after a single dose of intramuscular vaccination in mice. This
352 is consistent with our previous findings using the same mouse vaccination model¹⁷. The low
353 antibody titres for unadjuvanted QIV correlated well with low T cell responses (IL-4 and IFN- γ
354 ELIs) as well as inadequate protection against virus infection, implied by high levels of
355 replicating virus in lungs upon intranasal IVR-180 challenge. These animals also showed most body
356 weight loss and high levels of inflammatory cytokines in their lungs post infection, suggesting the

357 recruitment of immune cells to aid in control/clearance of the virus. QIV formulated with either of
358 two LNPs and/or further combined with either SDI or IMDQ-PEG-Chol as adjuvant, show a boosted
359 total IgG response and a better control over virus replication by day 5 post infection. However, the
360 administration of individual or combination adjuvants directed the B cell class switch as well as T
361 cell responses in vaccinated mice. Upon a single vaccination, SDI induced a balanced IgG1/IgG2a
362 response, IMDQ-PEG-Chol directed more towards an IgG2a response and the combination of the
363 two skewed completely towards IgG2a, when formulated into S or K LNPs, suggesting very strong
364 class switching events driven by this combination of adjuvants and consistent with our previous
365 findings. Interestingly, the combination of the two adjuvants SDI and IMDQ-PEG-Chol induces a
366 balanced type-I and -II T cell responses as suggested by a balanced IL-4 and IFN- γ release upon
367 antigenic restimulation. Therefore, the combination of IMDQ-PEG-Chol and SDI in LNP
368 formulations results in a balanced Th1/Th2 which results in complete type 1 skewing when antibody
369 responses are considered.

370 Interestingly, S-Ac7-Dog LNPs were found to be more immunogenic than K-Ac7-Dsa LNPs in
371 inducing both humoral and cellular responses in corresponding groups. Yet, vaccination with empty
372 S-Ac7-Dog LNPs resulted in lack of protection from morbidity in challenged mice. Remarkably, S-
373 Ac7-Dog(-) + IMDQ-PEG-Chol vaccination also resulted in lack of protection from morbidity after
374 infection, with body weight loss comparable to unvaccinated/PBS control animals. This lack of
375 protection from morbidity was accompanied by enhanced inflammatory cytokine responses including
376 interleukins IL-4, IL-5, IL-6 and IL-13, interferon gamma (IFN- γ) as well as chemokine GMCSF. In
377 contrast, when S-Ac7-Dog LNPs were combined with SDI, inflammation is relatively reduced in
378 infected lungs as suggested by the chemokines/cytokines levels. The differences might plausibly be
379 attributed by the lower stability of S-Ac7-Dog than K-Ac7-Dsa lipids in respective LNPs, which
380 might be stabilized by addition of an opposite charged SDI molecules. However, we need additional
381 experiments to confirm this.

382 Overall, we compared two different lipid compositions in LNP formulations, empty or loaded with
383 individual or combination adjuvants. Different combinations affected both B and T cell responses
384 along with vaccine/adjuvant/LNP-dependent inflammation in single vaccinated mice upon virus
385 infection. The negatively charged SDI might stably interact with cationic lipid moieties providing
386 more stability to the entire structure and thereby reducing related inflammation in infected animals.
387 The immunogenicity and protection data in mice combined with the cytokine/chemokine induction
388 indicates that lipid composition of LNPs used in vaccines is important and can skew host immune
389 responses to subsequent infection, and therefore is important for vaccine safety and efficacy.

390

391 **Methods and Reagents**

392 A list of reagents used in the study is provided in supplementary table I.

393 **Cell lines**

394 Madin-Darby canine kidney (MDCK) cell line was maintained in Dulbecco's Modified Eagle
395 Medium (DMEM) supplemented with 10% Fetal bovine serum (FBS) and 1X antibiotics (penicillin/
396 streptomycin).

397 **QIV vaccine**

398 Quadrivalent Inactivated influenza vaccine (FLUCALVEX 2018/2019 season Lot 252681) was
399 obtained from Seqirus. The vaccine consists of MDCK-grown two Influenza A and two B viruses-
400 A/ Singapore/GP1908/2015 IVR-180 (H1N1) (A/Michigan/45/ 2015-like virus), A/North
401 Carolina/04/2016 (H3N2) (A/ Singapore/INFIMH-16-0019/2016 -like virus), B/Iowa/06/2017
402 (B/Colorado/06/2017-like virus) and B/Singapore/INFTT-16- 0610/2016 (B/Phuket/3073/2013-like
403 virus).

404 **SDI-RNA**

405 The SDI-RNA (or SDI) was *in vitro* transcribed as described in our recent study.

406 **Lipid nanoparticle (LNP) fabrication:**

407 1 μ g SDI or SDI equivalent was encapsulated in LNPs by rapid mixing under vigorous stirring of an
408 acetate buffer (5 mM, pH 4.5) containing SDI with an ethanolic solution containing the ionizable
409 lipid S-Ac7-Dog or K-Ac7-Dsa (to obtain S-Ac7-Dog and K-Ac7-Dsa LNPs respectively),
410 cholesterol, 1,2-dioleoyl-n-glycero-3-phosphoethanolamine (DOPE) and a poly(ethylene glycol)-
411 lipid (DSG-PEG; PEG had an MW of 2 kDa) at a 50:38.5:10:1.5 ratio. After mixing, LNP were
412 dialyzed against 1X PBS to get rid of ethanol and the pH was adjusted to 7.4. An N/P (ionizable
413 Nitrogen atoms of the ionizable lipid to anionic Phosphor atoms of SDI) molar ratio of 5:1 was
414 targeted.

415 **LNP characterization:**

416 The diameter and polydispersity index (PDI) of LNPs was measured with Dynamic light scattering
417 (DLS) at physiological pH. Each sample was measured in triplicates and a cumulative average of z
418 average and PDI was calculated. For ELS, each sample was appropriately diluted in HEPES buffer

419 and measurements were taken in triplicates. The Zeta potential was calculated for all samples based
420 on the Smoluchowski equation.

421 **Vaccine-adjuvant preparation and administration**

422 For each animal, 1.5mg HA equivalent of QIV was mixed with empty or SDI-encapsulating S-Ac7-
423 Dog or K-Ac7-Dsa LNPs, with or without 100 g IMDQ-PEG-Chol (equivalent to 10 g core
424 IMDQ), and vortexed for 30 seconds (s). Adjuvant doses were chosen based on our previously
425 published work with these adjuvants^{17,30}. Unadjuvanted or adjuvanted QIV, with or without LNP
426 formulations, was administered intramuscularly in a total of 50 μ l per mouse, in the right hind leg.
427 The control group were administered with equal volume of PBS instead of vaccine or vaccine \pm
428 adjuvant \pm LNP mixture. All animals received only one dose of vaccine without any further boosters.

429 **IVR-180 virus**

430 A/Singapore/GP1908/2015 IVR-180 (H1N1) was grown in 8-days old embryonated chicken eggs
431 and was titrated by plaque assay on pre-seeded MDCK cells. The half-lethal dose of virus needed to
432 kill mice (LD₅₀) was calculated based on intranasal infections in 6-8 weeks old naïve female BALB/c
433 mice using 10-fold serial dilutions of the virus.

434 **Mouse model**

435 The study was performed on 6–8-week-old female BALB/c mice strains obtained from Charles River
436 Laboratories, MA. The mice were housed with food and water ad libitum in a pathogen-free facility
437 at Icahn School of Medicine at Mount Sinai, New York. All mice were vaccinated intramuscularly
438 (50 μ l; right hind leg; per mouse) and infected intranasally (in 50 μ l total volume per mouse) under
439 ketamine/xylazine anesthesia. All procedures were performed according to the protocols approved by
440 the Icahn School of Medicine at Mount Sinai Institutional Animal Care and Use Committee (IACUC
441 -PROTO202100007).

442 **Serum collection for serology**

443 Mice blood was collected by submandibular bleed 3 weeks post vaccination from all animals. The
444 blood was allowed to clot at 4°C for overnight. The serum was collected after a brief centrifugation
445 and was heat inactivated at 56°C for 30 min. The samples were stored at -20°C until further use.

446 **Enzyme-linked immunosorbent assay**

447 Enzyme-linked immunosorbent assay (ELISA) was performed to quantify the vaccine-specific IgG
448 titers in mice sera. Briefly, ELISA plates were coated with recombinant trimeric HA (derived from
449 the A/Michigan/45/2015 H1N1 virus, which is closely related to IVR-180; as previously described¹⁷,
450 equivalent to 2 μ g H1N1-HA/ml, in bicarbonate buffer and left overnight at 4°C. Plates were washed
451 three times with 1X PBS and incubated in 100 μ l blocking buffer per well (5% fat-free milk in PBST
452 (1X PBS + 0.1% Tween20)) for 1 hour (h) at room temperature (RT). In the meantime, the serum
453 samples were serially diluted 3-fold, starting with 1:100 dilution, in the blocking buffer and 50 μ l of
454 each sample dilution was incubated on HA-coated ELISA plates for overnight at 4°C. The following
455 day, the plates were washed three times with PBST and incubated with 100 μ l of diluted horse radish
456 peroxidase (HRP)-conjugated anti-mouse secondary total IgG (1:5000) or IgG1 (1:2000) or IgG2a
457 (1:2000) antibodies, for 1h at RT. Finally, the plates were washed three times in PBST and incubated
458 with 100 μ l of tetramethylbenzidine (TMB) substrate at RT until the blue color appeared. The
459 reaction was terminated with 50 μ l of 1M sulfuric acid (H₂SO₄), and the absorbance was measured at
460 450nm and 650nm wavelengths using BIOTEK ELISA plate reader.

461 **Hemagglutination inhibition assay (HAI)**

462 Mice sera collected 3 weeks post-vaccination were treated with 4 volumes of receptor destroying
463 enzyme (RDE) at 37°C overnight, followed by treatment with 5 volumes of 1.5% sodium citrate at
464 56°C, 30 min. Thus obtained 1:20-diluted serum samples were further serially diluted in a
465 transparent V-bottom 96-well plate and incubated with 4HA units per well of IVR-180 virus for 30
466 min at RT, followed by addition of 0.5% chicken red blood cells for 40 min at 4°C. The results were
467 recorded as HAI titers.

468 **Enzyme-linked immunosorbent spot**

469 Mice were vaccinated with different combinations of QIV \pm adjuvant \pm LNP and the spleens were
470 harvested 10 days post-vaccination from all vaccinated as well as unvaccinated animals. The spleens
471 were collected in 5ml RPMI-1640 media supplemented with 2% FBS and 1X penicillin/streptomycin
472 and kept on ice. A single cell suspension of splenocytes was obtained by homogenizing the spleens
473 against a 70 μ m strainer. Interferon gamma (IFN- γ) or Interleukin-4 (IL-4) enzyme-linked
474 immunosorbent spot (ELIspot) assays were performed using 10⁵ splenocytes per well in a 96-well
475 Polyvinylidene difluoride (PVDF) ELIspot plates, precoated with IFN- γ or IL-4 capture antibodies,
476 respectively, according to manufacturer's protocol. Splenocytes were unstimulated or restimulated
477 either with hemagglutinin (HA-H1N1) overlapping 15-mer peptides or whole live IVR-180 (H1N1)
478 virus and incubated overnight in 37°C incubator. The wells were washed thrice with water to get rid

479 of cells and incubated with 100 μ l of biotinylated polyclonal detection antibody against IFN- γ or IL-4
480 for 1.5h at RT, followed by an incubation with streptavidin-HRP conjugated antibody for 1h at RT.
481 The plates were finally incubated with 100 μ l of the substrate for 1h in dark, followed by thorough
482 washing under tap water multiple times. The plates were air dried in dark and the number of spots in
483 each well were manually counted using a dissection microscope. The results were represented as
484 number of IFN- γ or IL-4 producing splenocytes per million splenocytes.

485 **Virus challenge**

486 100LD₅₀ of IVR-180 (18000 plaque forming units (PFU) per animal), was used for intranasal
487 infection in a final volume of 50 μ L per mouse. The virus challenge was performed under mild
488 anesthesia with ketamin/xylazine (intraperitoneal) as recommended by AICUC. The unvaccinated
489 but challenged group was used as a control in the experiment. Body weights were recorded every day
490 post-infection until lung harvest. The lungs were collected at 5 days post-infection (DPI) in 500 μ l 1X
491 PBS and homogenized using a tissue homogenizer. The lysate thus obtained was stored at -80°C for
492 viral titrations.

493 **Plaque assay**

494 Virus titrations were performed by plaque assays to quantify the replicating virus titers in the lungs
495 of vaccinated versus unvaccinated mice. The lung homogenate (or lysate) was 10-fold serially
496 diluted in 1X PBS and incubated on pre-seeded and pre-washed monolayers of MDCK cells for 1h in
497 an incubator, at 37°C, 5% CO₂ with gentle shaking every 5 min. The diluted samples were then
498 removed, and the monolayers were again briefly washed with 1ml 1X PBS. Lastly, 1ml of the
499 overlay mixture (2% oxoid agar and 2X minimal essential medium (MEM) supplemented with 1%
500 diethyl-aminoethyl (DEAE)-dextran and 1 mg/ml tosylamide-2- phenylethyl chloromethyl ketone
501 (TPCK)-treated trypsin) was added on top of the monolayers and incubated for 48 h in the incubator,
502 at 37°C, 5% CO₂. The plates were finally fixed in 4% formaldehyde. The overlay was removed, and
503 the plaques were immune-stained with IVR-180-postchallenge polyclonal serum, diluted 1:1000 in
504 blocking buffer. The plates were washed and incubated with 1:5000 dilution of horse radish
505 peroxidase (HRP)-conjugated anti-mouse secondary antibody for 1h at RT with gentle shaking.
506 Followed by a brief washing in 1X PBST, the plaques were finally visualized with True Blue
507 substrate and the number of plaques were counted and represented as PFU/ml.

508 **Multiplex ELISA**

509 Multiplex ELISA was performed for simultaneous measurements of different cytokines in the lung
510 homogenates from IVR-180-infected mice. The following cytokines were measured: Granulocyte
511 macrophage colony-stimulating factor (GMCSF), Interleukin (IL)-1 β , IL-4, IL-5, IL6, IL-12p70, IL-
512 13, IL-18 and Interferon gamma (IFN- γ). The assay was performed according to the manufacturer's
513 guidelines and the readings were recorded using Luminex 100/200 system.

514 **Software**

515 The schematic figures were created with BioRender.com. GraphPad Prism version 10 was used for
516 data visualization, analysis, graph plotting and statistical analysis.

517

518 **Data availability statement**

519 The original contributions in the study are included in the article/supplementary material. Further
520 inquiries can be directed to the corresponding author at *michael.schotsaert@mssm.edu*.

521 **Ethics statement**

522 The animal study was reviewed and approved by the Institutional Animal Care and Use Committee
523 (IACUC) at the Icahn School of Medicine at Mount Sinai, New York.

524 **Author contributions**

525 Conceptualization and study design: SJ and MS.

526 Methodology: SJ (viruses, infections, mouse immunization), AL, YC and TY (LNP fabrication and
527 characterization), SJ and GL (*in vitro* serological assays), SJ and GS (ELIspots), SJ (multiplex
528 ELISA).

529 Reagents: SJ, AL, TY, YC, AG-S, BG and MS.

530 Investigation and data analysis: SJ and MS.

531 First draft of the manuscript: SJ and MS.

532 Manuscript review and editing: all authors.

533 Funding acquisition: AG-S, BG, and MS.

534 All authors contributed to the article and approved the submitted version.

535 **Funding and Acknowledgement**

536 This study was partly funded by CRIPT (Center for Research on Influenza Pathogenesis and
537 Transmission), a NIH NIAID funded Center of Excellence for Influenza Research and Response
538 (CEIRR, contract number 75N93021C00014), by the NIAID funded SEM-CIVIC consortium to
539 improve influenza vaccines (contract number 75N93019C00051) and by NIAID grant P01AI097092
540 to AG-S. Influenza research in the M.S. lab is further supported by NIH/NIAID R21AI151229,
541 R44AI176894 and R21AI176069. BG acknowledges funding from the European Research Council
542 (ERC) under the European Union's Horizon 2020 research and innovation program (grant N
543 817938).

544 **Conflict of interest**

545 The AG-S laboratory has received research support from GSK, Pfizer, Senhwa Biosciences, Kenall
546 Manufacturing, Blade Therapeutics, Avimex, Johnson & Johnson, Dynavax, 7Hills Pharma,
547 Pharmamar, ImmunityBio, Accurius, Nanocomposix, Hexamer, N-fold LLC, Model Medicines,
548 Atea Pharma, Applied Biological Laboratories and Merck, outside of the reported work. A.G.-S. has
549 consulting agreements for the following companies involving cash and/or stock: Castlevax, Amovir,
550 Vivaldi Biosciences, Contrafект, 7Hills Pharma, Avimex, Pagoda, Accurius, Esperovax, Farmak,
551 Applied Biological Laboratories, Pharmamar, CureLab Oncology, CureLab Veterinary, Synairgen,
552 Paratus, Pfizer and Prosetta, outside of the reported work. A.G.-S. has been an invited speaker in
553 meeting events organized by Seqirus, Janssen, Abbott and AstraZeneca. A.G.-S. is inventor on
554 patents and patent applications on the use of antivirals and vaccines for the treatment and prevention
555 of virus infections and cancer, owned by the Icahn School of Medicine at Mount Sinai, New York.
556 The MS laboratory received unrelated research support as sponsored research agreements from
557 ArgenX BV, Phio Pharmaceuticals, 7Hills Pharma LLC and Moderna. The remaining authors
558 declare that the research was conducted in the absence of any commercial or financial relationships
559 that could be construed as a potential conflict of interest.

560

561 **Supplementary Table:**

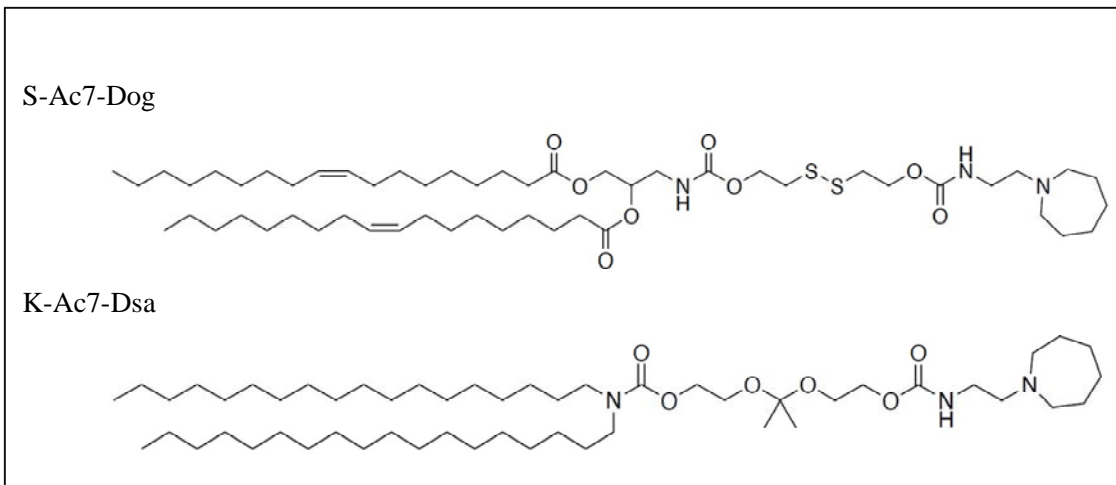
Reagent	Brand	Catalogue number
DMEM	Corning	10013-CV
RPMI 1640	Gibco	22400089
Penicillin/streptomycin	Corning	30002-CI
Goat HRP-conjugated secondary Anti-mouse IgG antibody	Abcam	Ab6823
Anti-mouse IgG1-HRP secondary antibody	Invitrogen	PA174421
Anti-mouse IgG2a-HRP secondary antibody	Invitrogen	A10685
TMB substrate	BD OptEIA	555214
KPL true blue substrate	Sera care	5510-0050
70µm strainer	BD	352340
Peptivator H1-HA peptide	MiltenyiBiotech	130-099-803
Oxoid agar	Thermofisher	LP0028B
EMEM	BioWhittaker	12684F
TPCK	Sigma	T4376
10% methanol-free formaldehyde	Polysciences	040181
2M Sulfuric acid	Thermo fisher	S25898
Mouse IFN- γ ELISPOT kit	RnD systems	EL485
Mouse IL-4 ELISPOT kit	RnD systems	EL404
ELISA NUNC-maxisorp plates	Invitrogen	44240421
Th1/Th2 Cytokine 11-Plex Mouse ProcartaPlex™ Panel	Invitrogen	EPX110-20820-901

562

563 **Supplementary table I:** List of reagents and kits used in the study.

564

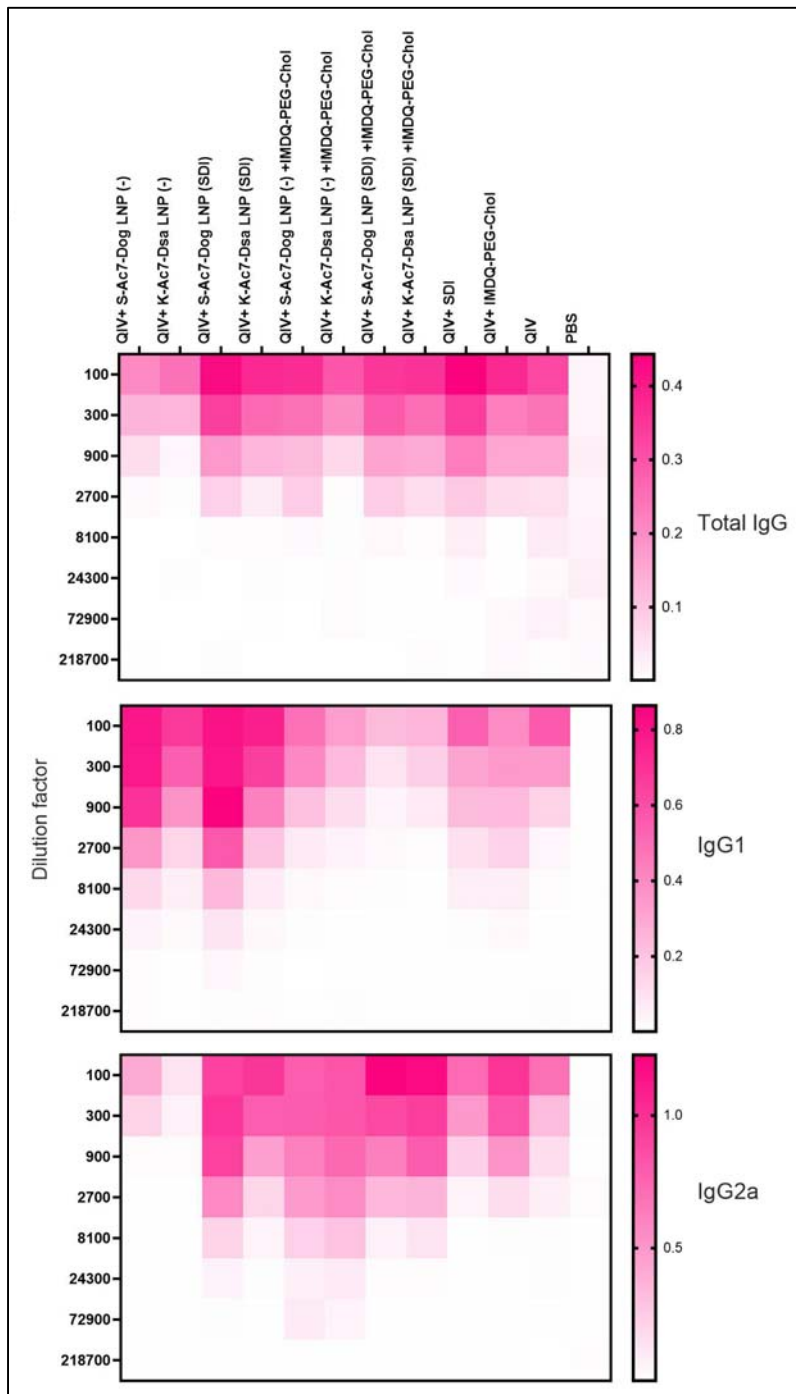
565 **Supplementary Figures:**



566

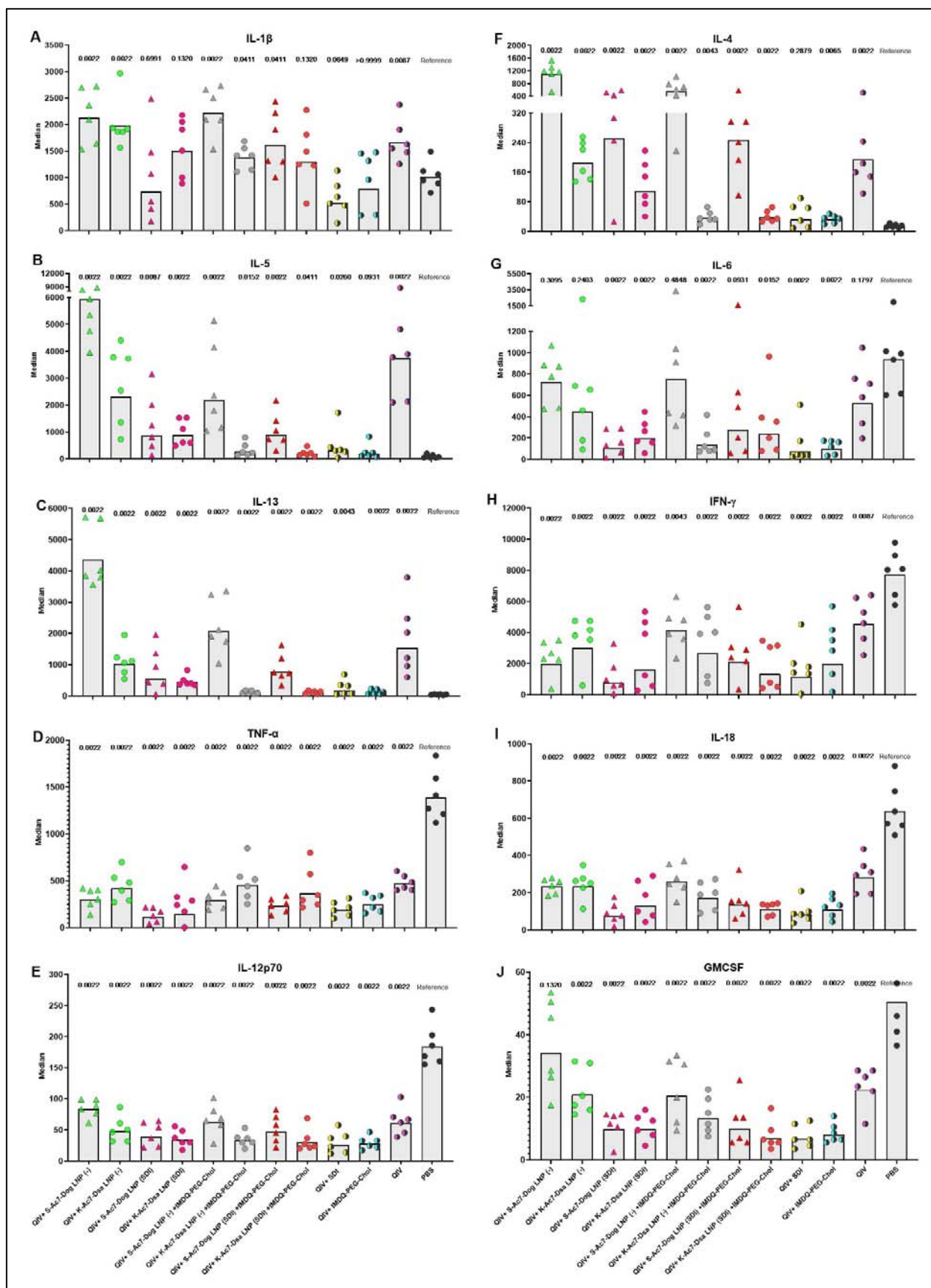
567

568 **Supplementary figure 1:** Chemical structure of in-house synthesized ionizable lipids- S-Ac7-Dog
569 and K-Ac7-Dsa lipids, comprising a disulfide bond that can be cleaved by reduction and a ketal bond
570 that can be cleaved by acidic pH, respectively.



571

572 **Supplementary figure 2:** Heatmap showing mean OD450 ELISA values (n=5 per group) plotted
573 against serum dilutions for total IgG, IgG1 and IgG2a. 6-8-week female BALB/c mice were
574 vaccinated with QIV with and without IMDQ-PEG-Chol and formulated into empty or SDI-
575 encapsulating S or K LNPs. Serum was collected 3 weeks post-vaccination by submandibular bleed.
576 Total IgG, IgG1 and IgG2a titers were quantified by ELISA with 3-fold serum dilutions starting with
577 1:100, for H1 HA specific antibodies.



579 **Supplementary figure 3:** All lungs from unvaccinated and vaccinated animals were collected at 5
580 days post infection and the cytokine levels were quantified by multiplex ELISA. Levels of **(A)** IL-
581 1β , **(B)** IL-5, **(C)** IL-13, **(D)** TNF- α , **(E)** IL-12 p70, **(F)** IL-4, **(G)** IL-6, **(H)** IFN- γ , **(I)** IL-18 and **(J)**
582 GMCSF, for n=6 animals per group are represented as geometric mean \pm geometric SD, where each
583 data point corresponds to individual mouse. Statistical analysis was performed using two-sided Mann
584 Whitney U test. The p values shown are calculated in reference to the virus-challenged unvaccinated
585 group (denoted as PBS).

586

587

588

589

590 **References:**

- 591 1. Cox RJ, Brokstad KA, Ogra P. Influenza virus: immunity and vaccination strategies. Comparison
592 of the immune response to inactivated and live, attenuated influenza vaccines. *Scand J Immunol.*
593 2004;59(1):1-15. doi:10.1111/j.0300-9475.2004.01382.x
- 594 2. Hannoun C. The evolving history of influenza viruses and influenza vaccines. *Expert Rev
595 Vaccines.* 2013;12(9):1085-1094. doi:10.1586/14760584.2013.824709
- 596 3. Kim H, Webster RG, Webby RJ. Influenza Virus: Dealing with a Drifting and Shifting Pathogen.
597 *Viral Immunol.* 2018;31(2):174-183. doi:10.1089/vim.2017.0141
- 598 4. Boni MF. Vaccination and antigenic drift in influenza. *Vaccine.* 2008;26 Suppl 3(Suppl 3):C8-
599 14. doi:10.1016/j.vaccine.2008.04.011
- 600 5. De Jong JC, Rimmelzwaan GF, Fouchier RA, Osterhaus AD. Influenza virus: a master of
601 metamorphosis. *J Infect.* 2000;40(3):218-228. doi:10.1053/jinf.2000.0652
- 602 6. Mooij P, Mortier D, Aartse A, et al. Vaccine-induced neutralizing antibody responses to seasonal
603 influenza virus H1N1 strains are not enhanced during subsequent pandemic H1N1 infection.
604 *Front Immunol.* 2023;14:1256094. doi:10.3389/fimmu.2023.1256094
- 605 7. Petrie JG, Ohmit SE, Truscon R, et al. Modest Waning of Influenza Vaccine Efficacy and
606 Antibody Titers During the 2007-2008 Influenza Season. *J Infect Dis.* 2016;214(8):1142-1149.
607 doi:10.1093/infdis/jiw105
- 608 8. Hsu JP, Zhao X, Chen MIC, et al. Rate of decline of antibody titers to pandemic influenza A
609 (H1N1-2009) by hemagglutination inhibition and virus microneutralization assays in a cohort of
610 seroconverting adults in Singapore. *BMC Infect Dis.* 2014;14(1):414. doi:10.1186/1471-2334-14-
611 414
- 612 9. Palese P, García-Sastre A. Influenza vaccines: present and future. *J Clin Invest.* 2002;110(1):9-
613 13. doi:10.1172/JCI15999
- 614 10. Harding AT, Heaton NS. Efforts to Improve the Seasonal Influenza Vaccine. *Vaccines (Basel).*
615 2018;6(2):19. doi:10.3390/vaccines6020019
- 616 11. Coutelier JP, van der Logt JT, Heessen FW, Warnier G, Van Snick J. IgG2a restriction of murine
617 antibodies elicited by viral infections. *J Exp Med.* 1987;165(1):64-69. doi:10.1084/jem.165.1.64
- 618 12. Coutelier JP, van der Logt JT, Heessen FW, Vink A, van Snick J. Virally induced modulation of
619 murine IgG antibody subclasses. *J Exp Med.* 1988;168(6):2373-2378.
620 doi:10.1084/jem.168.6.2373
- 621 13. Hovden AO, Cox RJ, Haaheim LR. Whole influenza virus vaccine is more immunogenic than
622 split influenza virus vaccine and induces primarily an IgG2a response in BALB/c mice. *Scand J
623 Immunol.* 2005;62(1):36-44. doi:10.1111/j.1365-3083.2005.01633.x
- 624 14. Barackman JD, Ott G, O'Hagan DT. Intranasal immunization of mice with influenza vaccine in
625 combination with the adjuvant LT-R72 induces potent mucosal and serum immunity which is

626 stronger than that with traditional intramuscular immunization. *Infect Immun.* 1999;67(8):4276-
627 4279. doi:10.1128/IAI.67.8.4276-4279.1999

628 15. Moran TM, Park H, Fernandez-Sesma A, Schulman JL. Th2 responses to inactivated influenza
629 virus can Be converted to Th1 responses and facilitate recovery from heterosubtypic virus
630 infection. *J Infect Dis.* 1999;180(3):579-585. doi:10.1086/314952

631 16. Hovden AO, Cox RJ, Madhun A, Haaheim LR. Two doses of parenterally administered split
632 influenza virus vaccine elicited high serum IgG concentrations which effectively limited viral
633 shedding upon challenge in mice. *Scand J Immunol.* 2005;62(4):342-352. doi:10.1111/j.1365-
634 3083.2005.01666.x

635 17. Jangra S, Laghlali G, Choi A, et al. RIG-I and TLR-7/8 agonists as combination adjuvant shapes
636 unique antibody and cellular vaccine responses to seasonal influenza vaccine. *Front Immunol.*
637 2022;13:974016. doi:10.3389/fimmu.2022.974016

638 18. Visciano ML, Tagliamonte M, Tornesello ML, Buonaguro FM, Buonaguro L. Effects of
639 adjuvants on IgG subclasses elicited by virus-like particles. *J Transl Med.* 2012;10:4.
640 doi:10.1186/1479-5876-10-4

641 19. Huber VC, McKeon RM, Brackin MN, et al. Distinct contributions of vaccine-induced
642 immunoglobulin G1 (IgG1) and IgG2a antibodies to protective immunity against influenza. *Clin
643 Vaccine Immunol.* 2006;13(9):981-990. doi:10.1128/CVI.00156-06

644 20. Pulendran B, S Arunachalam P, O'Hagan DT. Emerging concepts in the science of vaccine
645 adjuvants. *Nat Rev Drug Discov.* 2021;20(6):454-475. doi:10.1038/s41573-021-00163-y

646 21. Snapper CM, Paul WE. Interferon-gamma and B cell stimulatory factor-1 reciprocally regulate
647 Ig isotype production. *Science.* 1987;236(4804):944-947. doi:10.1126/science.3107127

648 22. Lee Y, Jeong M, Park J, Jung H, Lee H. Immunogenicity of lipid nanoparticles and its impact on
649 the efficacy of mRNA vaccines and therapeutics. *Exp Mol Med.* 2023;55(10):2085-2096.
650 doi:10.1038/s12276-023-01086-x

651 23. Tenchov R, Bird R, Curtze AE, Zhou Q. Lipid Nanoparticles—From Liposomes to mRNA
652 Vaccine Delivery, a Landscape of Research Diversity and Advancement. *ACS Nano.*
653 2021;15(11):16982-17015. doi:10.1021/acsnano.1c04996

654 24. Schoenmaker L, Witzigmann D, Kulkarni JA, et al. mRNA-lipid nanoparticle COVID-19
655 vaccines: Structure and stability. *Int J Pharm.* 2021;601:120586.
656 doi:10.1016/j.ijpharm.2021.120586

657 25. Zhong Z, Chen Y, Deswarth K, et al. Lipid Nanoparticle Delivery Alters the Adjuvanticity of the
658 TLR9 Agonist CpG by Innate Immune Activation in Lymphoid Tissue. *Adv Healthc Mater.*
659 Published online September 29, 2023:e2301687. doi:10.1002/adhm.202301687

660 26. Zhang C, Ma Y, Zhang J, et al. Modification of Lipid-Based Nanoparticles: An Efficient
661 Delivery System for Nucleic Acid-Based Immunotherapy. *Molecules.* 2022;27(6):1943.
662 doi:10.3390/molecules27061943

663 27. Lamoot A, Jangra S, Laghlali G, et al. Lipid Nanoparticle Encapsulation Empowers Poly(I:C) to
664 Activate Cytoplasmic RLRs and Thereby Increases Its Adjuvanticity. *Small*. Published online
665 October 22, 2023:2306892. doi:10.1002/smll.202306892

666 28. Martínez-Gil L, Goff PH, Hai R, García-Sastre A, Shaw ML, Palese P. A Sendai virus-derived
667 RNA agonist of RIG-I as a virus vaccine adjuvant. *J Virol*. 2013;87(3):1290-1300.
668 doi:10.1128/JVI.02338-12

669 29. Patel JR, Jain A, Chou Y ing, Baum A, Ha T, García-Sastre A. ATPase-driven oligomerization
670 of RIG-I on RNA allows optimal activation of type-I interferon. *EMBO Rep*. 2013;14(9):780-
671 787. doi:10.1038/embor.2013.102

672 30. Jangra S, De Vrieze J, Choi A, et al. Sterilizing Immunity against SARS-CoV-2 Infection in
673 Mice by a Single-Shot and Modified Imidazoquinoline TLR7/8 Agonist-Adjuvanted
674 Recombinant Spike Protein Vaccine. *bioRxiv*. Published online October 23,
675 2020:2020.10.23.344085. doi:10.1101/2020.10.23.344085

676